JOURNAL OF Applied Polymer SCIENCE

Conductive Composites from Polyaniline and Polyurethane Sulphonate Anionomer

Riblu Deka, Montu Moni Bora, Madhab Upadhyaya, Dilip Kumar Kakati
Department of Chemistry, Gauhati University, Assam 781014, India
Correspondence to: D. K. Kakati (E-mail: dilip_kakati2003@yahoo.co.in)

ABSTRACT: The present work describes the synthesis of conductive composite of polyurethane sulphonate anionomer (PUSA) and para toluene sulphonic acid doped polyaniline (PANI–PTSA). HCl-doped PANI was synthesized by chemical oxidative polymerization of aniline in HCl, which was converted to PANI–EB by treatment with NH_4OH. PTSA doped PANI was synthesized from EB-PANI by redoping with PTSA solution. PUSA was synthesized from 4, 4′-diphenylmethanediisocyanate (MDI), polypropylene glycol (PPG), 1,4-butanediol (BD), and ionic diol SDOL. The composite was prepared by mixing of the solutions of two polymer components in DMF and then solution casting. The products were characterized and analyzed by UV-Vis and FTIR spectroscopy, thermogravimetry, differential scanning calorimetry and scanning electron microscopy. The conductivity was found to increase by 100 times with concomitant decrease in percolation threshold when polyurethane was replaced by PUSA in the composite for the same amount of polyaniline. The composite film was thermally stable upto ~300°C. © 2014 Wiley Periodicals, Inc. J. Appl. Polym. Sci. **2015**, *132*, 41600.

KEYWORDS: composites; conducting polymers; thermogravimetric analysis

Received 14 September 2013; accepted 4 October 2014
DOI: 10.1002/app.41600

INTRODUCTION

The discovery of iodine doped conducting polyacetylene, opened the floodgates of research works focused on developing new intrinsically conducting polymers, like polyaniline (PANI), polypyrrole, polythiophene, poly(*p*-phenylene) etc., for their applications in rechargeable batteries, bio- and chemical sensors, transducers, actuators, antistatic coatings, EMI-shielding, anticorrosive paints etc.[1–4] In the class of intrinsically conducting polymers, PANI has been one of the most extensively investigated due to its ease of preparation, chemical and thermal stability, simple doping and dedoping processes and use of cheap monomer. However the processibility of the emeraldine salt (ES) form of PANI, which is the conductive form, is somewhat troublesome due to its poor solubility in common organic solvents and it is not fusible as well. To overcome this problem, different strategies have been attempted, like introduction of lateral groups to the chain, block copolymerization and preparation of blend or composite with other polymers. Materials thus obtained, however, do not have the same level of conductivity as of the pure ES. The insertion of substituent for example, either in aromatic ring[5–8] or in the nitrogen atom[9–12] can improve solubility, but adversely affects the conductivity due to the chain twisting caused by steric effects that decreases the effective conjugation length. The combination of PANI segments with block of another polymer has also been attempted, like the grafting of PANI glycol[13] or poly acrylic acid[14] on to PANI. The preparation of blends and composites of conducting and conventional polymers has also generated a lot of research interest in the academia and industries.[15,16] This is because such blends and composites open the possibility of combining the good mechanical properties and processibility of conventional polymer with the conducting properties of the conducting polymer. However, the low miscibility of the conducting polymer chains in the host matrix is still an area of concern. There are attempts to enhance the compatibility by choosing a host polymer which can have covalent, hydrogen bonding or ionic interactions with the conducting polymer.

Polyurethane (PU) is a versatile class of polymer displaying all kinds of mechanical behavior, from hard plastics to soft rubbers. This is due to the different chemical compositions that can be achieved by simply altering the nature of the diol and diisocyanate used for the synthesis of PU. Segmented PUs could be designed in such a way that chemically different blocks could be bound by joining one —OH terminated segment with an —NCO terminated prepolymer with no by-products.[17] As the PU could be synthesized in a variety of compositions, it provides an opportunity to design conducting materials with a wide range of physical properties. The urethane linkages (—NHCOO—) of PU may also enhance the compatibility with PANI through hydrogen bonding. Malmonge et al.[18] synthesized flexible and free standing

Table I. Amount of Reactants Used for the Synthesis of Polyurethane Sulphonate Anionomers MDI : PPG : (BD + SDOL) 3 : 1 : 2

Code of ionomer	MDI (g)	PPG (g)	BD (g)	SDOL (g)
$PUSA_{25}$	3.34	4.4	0.6	0.43
$PUSA_{50}$			0.4	0.86
$PUSA_{75}$			o.2	1.29
$PUSA_{100}$			0.0	1.72

PU-PANI films and observed an increase in doping efficiency and conductivity by swelling of the film in DMF. Optically active core–shell PU-PANI composites with a PU-core and PANI-shell were synthesized by an electrochemical method.[19] Rodrigues et al.[20,21] attempted to enhance the compatibility between PU and PANI through interpenetrating polymer networks. The synthesis of composites from carboxylated PU grafted with PANI was investigated by Abbati et al.[22] Blends of PU and PANI-DBSA dispersions were studied by Kwon et al.[23] for their dynamic, mechanical, electrical and antistatic properties. A polymeric steric stabilizer poly (N-vinyl pyrrolidone) was used by Stejskal et al.[24] to prepare a composite from PU-latex and PANI. They observed a maximum conductivity of 10^{-2} S/cm and mechanical properties typical of elastomers in the composite. The extent of PANI dispersed in the TPU-polymer matrix strongly influenced the conductivity in the composites of DBSA-doped PANI and thermoplastic PU[25] Chien-Yu[26] and coworkers synthesized conductive core–shell particles based on PU/PANI and PU-poly (methyl methacrylate)/PANI and investigated their conducting and morphological properties. PANI and PU-prepolymer modified diglycidyl ether of bisphenol-A epoxy were used to prepare toughened semiconductive PANI/PU-epoxy nanoblends.[27,28] An exhaustive list of works on conductive blends and composites of PU with varieties of conducting materials has been compiled by Gurunathan et al.[29] PU ionomers are variants of PUs which contain a small percentage of ionic groups either in the backbone or pendent to the backbone.[30–33] Cao et al.[34] reported that the compatibility between the PANI and conventional polymer could be increased through the insertion of counter ions among the chains. PU anionomers with negatively charged groups may enhance the compatibility with the ES form of PANI through coulombic interactions. To the best of our knowledge there is very little reported work on blends or composites of PANI with PU anionomers. The present work describes the synthesis and characterization of conductive composites of PU sulphonate anionomer (PUSA) and para toluene sulphonic acid (PTSA) doped PANI (PANI.PTSA).

EXPERIMENTAL

Materials

Poly propylene glycol (PPG) $M_w = 1000$(Aldrich, USA) was purified by heating at 100°C for 6 h under vacuum. 1, 4-Butanediol (BD) (Aldrich, USA) was purified by distillation under reduced pressure. 4, 4′-diphenylmethanediisocyanate (MDI) (Aldrich, USA) and 3-chloropropane-1, 2-diol (CPD) (Aldrich, USA), potassium sulphite (Aldrich, USA) and PTSA (MERCK, Germany) were used as received. Aniline (MERCK, Iidia) was purified by double distillation under reduced pressure and stored in dark before use. The organic solvents like DMSO, THF, DMF, chloroform and toluene (MERCK, Iidia) were purified by standard procedures.[35]

Synthesis

Synthesis of Potassium-S-1, 2-Dihydroxypropylsulfonate (SDOL). Potassium-S-1, 2-dihydroxypropylsulfonate (SDOL) was synthesized by the procedure reported by Chui et al.[30] Potassium sulfite (4.74 g) and CPD (2.2 g) were dissolved separately in 5 mL water. The two solutions were mixed and refluxed gently for 4h and cooled. Unreacted CPD was removed by extraction with diethyl ether (2x5 mL). Water was then removed under reduced pressure and cooled. The resulting SDOL was extracted from the inorganic salt with DMSO (3x20 mL).The DMSO extracts were centrifuged for 8 minutes at 10,000 rpm. The solvent was then removed under reduced pressure to get viscous colourless oil. The oil was mixed with 3 mL of water followed by addition of ethanol (20 mL) to form an emulsion from which the product crystallized after standing for 2h at room temperature. The product was collected by filtration and washed with cold ethanol before being dried in a vacuum desiccator at room temperature.

Synthesis of PANI Emeraldine Salt. An aqueous solution (200 mL) of 1M HCl was prepared. 9.12 g ammonium persulphate (APS) was dissolved in 60 mL of 1M HCl and then cooled. 3.64 mL aniline was dissolved in the remaining 140 mL of 1M HCl also under ice cold condition. The APS solution was added slowly into aniline solution in 30 minutes with constant stirring and the stirring was continued for another 2h. It was then filtered, washed with dilute HCl and thereafter with distilled water and then dried in vacuum oven for 6h at 60°C. This is HCl doped PANI or emeraldine salt (ES-PANI). The emeraldine base form of PANI (EB-PANI) was prepared by treating it with 1M NH_4OH solution. The EB-PANI was re-doped with para toluene sulfonic acid (PTSA) by agitating it in 1M PTSA solution for 12h. It was then filtered and dried under vacuum to get PTSA doped PANI (PANI.PTSA).

Synthesis of PUSA. A solution of PPG (4.40 g) in 20 mL DMSO was added to MDI (3.34g) in 25mL DMSO over 10 minutes at 60°C under nitrogen atmosphere. The mixture was stirred for 1h at 70°C under nitrogen atmosphere. It was then cooled to 60°C and a solution of SDOL (1.72g in 25mL DMSO) was added dropwise over 10 minutes followed by addition of 0.02g of di-butyltindilaureate. The mixture was then heated for another 2h at 70°C. The resultant polymer ($PUSA_{100}$) was then precipitated in water. It was washed and dried in vacuum at room temperature. $PUSA_{75}$, $PUSA_{50}$, $PUSA_{25}$ and $PUSA_0$were also synthesized by the same procedure using BD along with SDOL, as chain extender. The different amount of reactants used for them are listed in Table I.

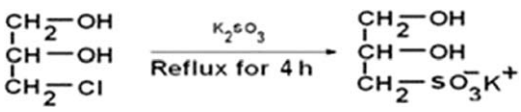

Scheme 1. Synthesis of SDOL.

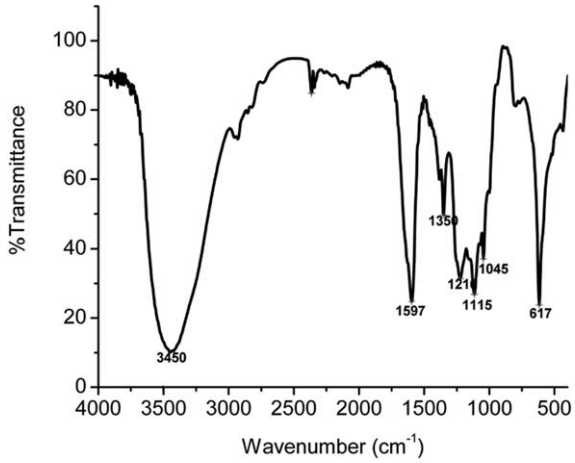

Figure 1. FTIR spectrum of SDOL.

Preparation of PUSA/ PANI Composite. The composites were prepared by solution casting process.[36] Out of the four solvents DMF, DMSO, NMP and THF tested for the purpose, DMF was found to be the most suitable for the following reasons: (a) deprotonation was observed when pre-doped PANI was dissolved in NMP, which was evident from the typical bluish colour instead of green colour of PANI in its conducting form.[37] Deprotonation was also observed in DMF but in more dilute solutions only, probably because of less basicity of DMF than NMP. (b) DMF has lower boiling point (153°C) than DMSO (182°C) and NMP (202°C) (c) $PUSA_{100}$ and composites were insoluble in THF. For the preparation of composites PU anionomer and PANI were separately dissolved in DMF. The two solutions were mixed and agitated for 2h to get a clear solution. It was then poured in a petri dish treated with 1% dichloro dimethyl silane solution in dichloromethane to cast a film. The solvent was evaporated under vacuum at 60°C. The film so obtained was dried and kept in vacuum desiccator for further characterization.

Characterization and Testing. The FTIR spectra of composites, PANI and PUSA were recorded in Perkin Elmer (USA) TXI FTIR spectrometer in the range 4000-400 cm^{-1}. FTIR spectrum of PANI was recorded in the form of KBr pellet while those of PUSA and composites were recorded in the form of thin films.

UV-visible spectra of PANI and the composites in DMF were recorded in SHIMADZU (Japan) 1800 UV-visible spectrophotometer in the range 200–800 nm. ^{1}HNMR spectra of samples were recorded in 300MHz BRUKER (USA) ADVANCE-III in D_6 DMSO.

The TGA of composites, PANI and PUSA were recorded in METTLER TOLEDO (UK), TGA/DSC 1, and STAR^e system in the range of 0°C to700°C, at the heating rate of 10°C/min under nitrogen atmosphere. The glass transition temperatures of $PUSA_{100}$ and $PUSA_{100}$-PANI.PTSA were measured in a PERKIN ELMER (Germany) 4000 thermogravimetric analyzer in the range of −40°C to 350°C, at a heating rate of 10°C/min.

The conductivities of the composites were measured at room temperature using the standard four probe electrode arrangement apparatus. The conductivity was calculated using the following formula: $\rho_o = (V/I)\ 2\pi S$, where ρ_o is resistivity, V is voltage difference, I is current passed and S is the sample thickness. The reciprocal of resistivity (i.e.1/ ρ_o) is the conductivity.

Morphological studies were done by SEM investigation of films with JSM-6360 (JEOL) (USA) scanning electron microscope. The observations were made at an accelerating voltage of 20 kV and films were coated with gold to avoid ionization of the samples. Field emission SEM was recorded in SIGMA-VP (ZEISS) (USA) scanning electron microscope at an accelerating voltage of 5 kV.

RESULTS AND DISCUSSION

Characterization of SDOL

SDOL was characterized on the basis of FTIR and ^{1}H NMR spectra and their comparison with reported results.

FTIR Analysis

The FTIR spectrum of SDOL is shown in Figure 1. The peak at 617 cm^{-1} is due to S—O deformations and the peak at 1045 cm^{-1} and a strong broad band centered at 1210 cm^{-1} are due to S—O stretching vibrations. The peak at 1597 cm^{-1} is due to —CH_2—bending absorption. The broad band centered at 3445 cm^{-1} is attributed to hydrogen bonded OH groups. The spectrum is in conformity with the reported data.[30]

^{1}H NMR of SDOL

^{1}H NMR spectrum of SDOL is presented in Figure 2 with the structure of SDOL shown in set. The peaks are assigned as follows: H (a) is a doublet centered at 4.85, H (b) is a triplet centered at 4.64ppm. H (c) is a multiplet centered at 3.76 ppm. Due to chiral prochiral centers on either side can effect geminal splitting of the protons. The protons at C-1 are split by the methine proton at the chiral center and experience a further splitting by the adjacent hydroxyl proton. Geminal splitting results in eight lines for the resonance pattern of H (d).

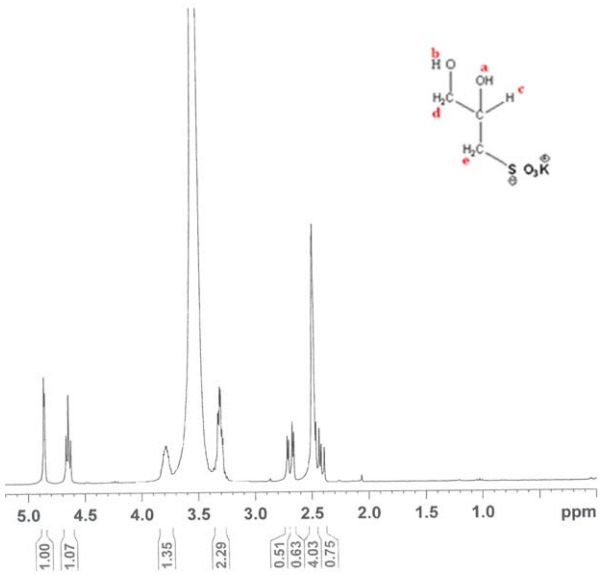

Figure 2. ^{1}H NMR spectra of SDOL. [Color figure can be viewed in the online issue, which is available at wileyonlinelibrary.com.]

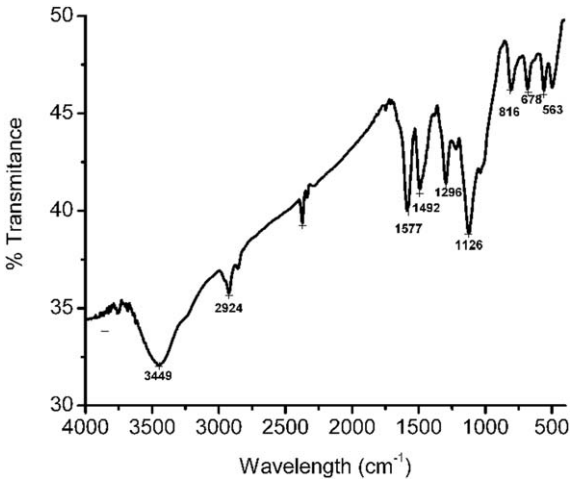

Figure 3. FTIR spectrum of PANI.

Similarly, the protons adjacent to sulphonate group H (e) appear as a multiplet, the reasons for which could not be explained. The integration values are in agreement with the number of hydrogen atoms in the compound. There are two prominent peaks due to presence of water and DMSO as contaminants.

Characterization and Studies on Composites

FTIR Analysis. The FTIR spectrum of PANI.PTSA is presented in Figure 3. The absorption bands at 1577 cm^{-1} and 1492 cm^{-1} correspond to quinoid and benzenoid ring deformations.[38] The broad band at 3448 cm^{-1} is due to N—H stretching, while the band at 2924 cm^{-1} is due to aromatic C—H stretching. The absorptions at 1296 cm^{-1} and 1126 cm^{-1} are due to the C—N stretching of the secondary aromatic amine and the stretching vibration of the sulphonic group (S═O) which are in good agreement with the values observed by Vicentini et al.[25] Further, the absorption at 813 cm^{-1} and 797 cm^{-1} are attributed to the C—H out of plane bending and para substituted aromatic ring vibrations.

FTIR spectra of PU ($PUSA_0$) and polyurethane sulphonate anionomer ($PUSA_{100}$) are shown in Figure 4. For $PUSA_0$ three

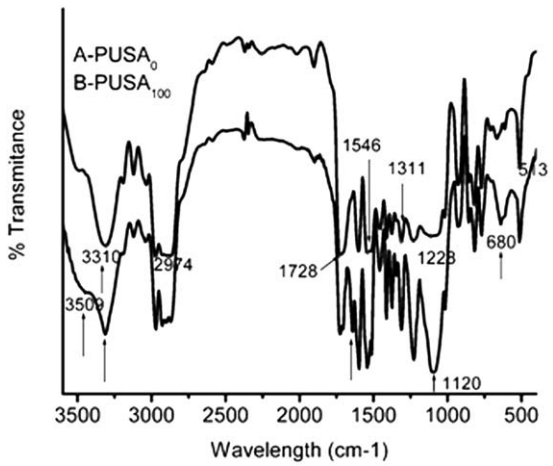

Figure 4. FTIR spectra of $PUSA_0$ and $PUSA_{100}$.

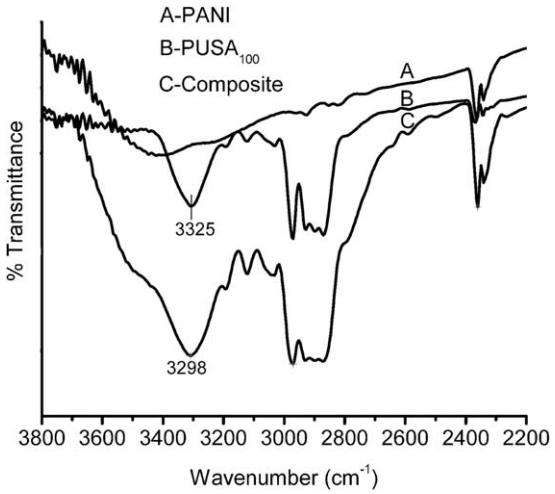

Figure 5. Terminal FTIR spectra of PANI, $PUSA_{100}$ and Composite showing N-H vibration.

important peaks, due to hydrogen bonded (N—H) stretching in urethane group, free carbonyl group of (C═O) urethane amide I, and hydrogen bonded carbonyl of urethane amide I, are observed at 3325 cm^{-1}, 1728 cm^{-1}, and 1720 cm^{-1} respectively. While the hydrogen bonded N—H stretching in $PUSA_{100}$ was observed at 3305 cm^{-1} the carbonyl absorptions were observed almost in the same region as in $PUSA_0$. Bands due to C—N stretching and N—H deformation (amide II band) at 1548 cm^{-1} and 1544 cm^{-1} were observed both in $PUSA_0$ and $PUSA_{100}$. A weak band, due to C—N stretching and N—H deformation (amide II band) is observed at 1228 cm^{-1} in $PUSA_0$ while a strong band is observed at 1224 cm^{-1} in $PUSA_{100}$ with a contribution from SO stretching. A peak observed for $PUSA_{100}$ at 680 cm^{-1} which is due to S—O deformation is absent at the FTIR spectrum of $PUSA_0$.

Figures 5 and 6 show the FTIR spectra of $PUSA_{100}$-PANI composite along with the spectra of PANI and $PUSA_{100}$ for comparison. The spectrum of composite shows all the major peaks due to the two constituents, although overlapping of certain absorptions in a relatively narrow range makes the interpretation

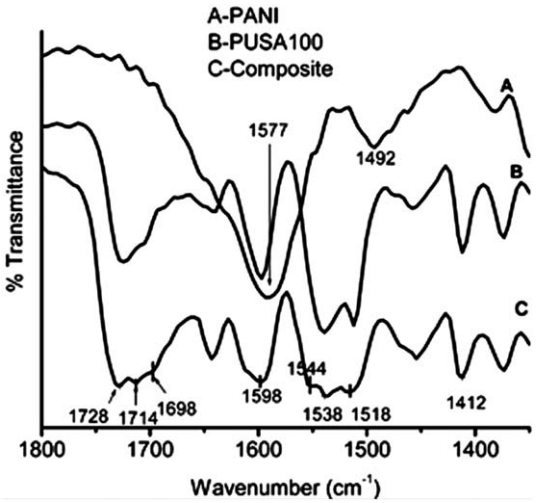

Figure 6. Mid FTIR spectra of PANI, $PUSA_{100}$, and Composite.

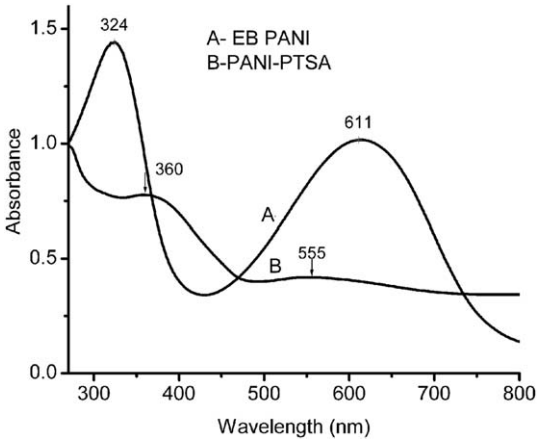

Figure 7. UV–Vis spectra of EB–PANI and PANI.PTSA.

somewhat difficult. FTIR spectroscopy is an important tool used to characterize the interactions between two or more components in a polymer blend or composite. In the FTIR-spectrum of PANI–PUSA composite, the important reasons to look for interactions are those exhibiting the —NH and >C=O peaks. The —NH— peak for PANI (3448 cm^{-1}) and $PUSA_{100}$ (3305 cm^{-1}) shifted to lower frequency (3298 cm^{-1}) in the composite, which is suggestive of certain degree of interactions between the two components. However, it needs to be emphasized the presence of —NH peaks in diverse environments, which is reflected in the broadening of the —NH peak [20]. The second region of interest is the one showing the absorptions due to urethane carbonyl group. However a number of absorptions such as those of the free carbonyl groups, those bonded to the —NH— groups of PUSA and PANI overlap in the relatively narrow range of 1670 cm^{-1} to 1730 cm^{-1}. This makes the interpretation difficult. However, the change in the nature of spectrum in this region for the composite is a clear indication of influence exerted by the —NH groups of PANI on the carbonyl group of $PUSA_{100}$.

UV–Visible Spectral Analysis

The UV–Vis spectra of EB–PANI and PANI.PTSA are presented in Figure 7. The UV–Vis spectrum of EB–PANI shows two strong absorption peaks at 611 nm and 324 nm. While the peak at 611 nm is attributed to excitation absorption due to benzenoid to quinoid transition, the peak at 324 nm is due to $\pi - \pi^*$ transition in the benzenoid ring.[14,15] When doped with PTSA a new peak appeared at ~380 nm. When protonation occurs, the quinoid ring becomes a semiquinoid radical cation and the observed peak is due to the polaronic structure. The peak observed at 611 nm for EB–PANI shows a blue shift in PANI.PTSA indicating partial oxidation of the polymer backbone.[16,17] The UV–Vis spectra of composites of $PUSA_{100}$, with 10, 20, and 25 wt % PANI.PTSA loading are represented in Figure 8. The UV–Vis spectra of the composites resemble the characteristic spectrum of PANI.PTSA. However, the intensity of the polaronic peak decreases with the decrease in amount of PANI in the composite.

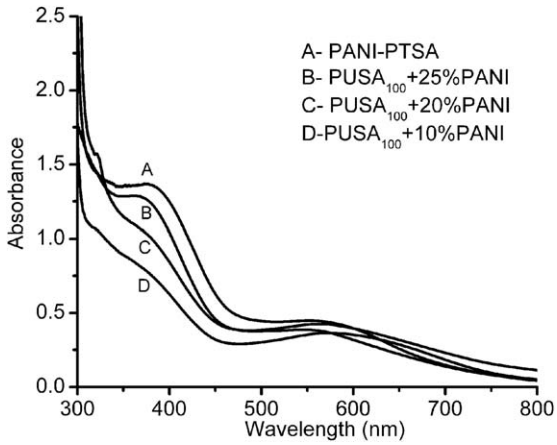

Figure 8. UV–Vis spectra of (A) PANI.PTSA, (B) 25 wt % of PANI.PTSA/$PUSA_{100}$, (C) 20 wt % of PANI.PTSA/$PUSA_{100}$, and (D) 10 wt % of PANI.PTSA/$PUSA_{100}$ composites.

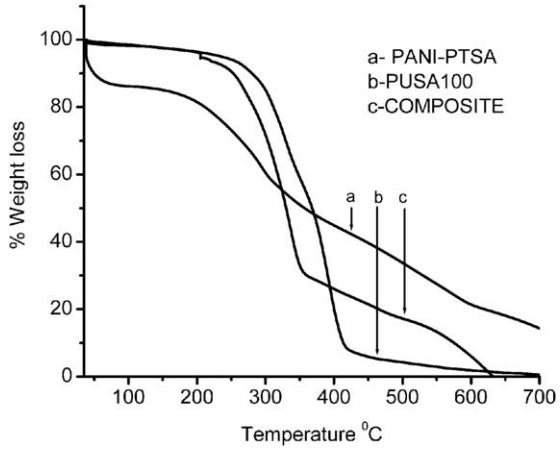

Figure 9. Thermogravimetric curves for (A) PANI.PTSA (B), $PUSA_{100}$, and (C) 30 wt % PANI.PTSA/$PUSA_{100}$.

Thermogravimetric Analysis

The TGA curves of PANI.PTSA, $PUSA_{100}$ and composites of 30 wt % of PANI.PTSA/$PUSA_{100}$ are shown in Figure 9. The TGA curves of PANI.PTSA exhibits three main reasons of degradation: first, in the region of room temperature −250°C (25% wt loss) which is attributed to the elimination of moisture and dopant anions in the sample.[39] The major weight loss of the samples in

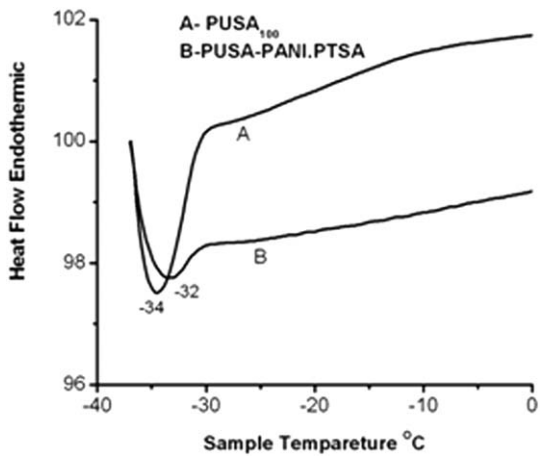

Figure 10. Low temperature DSC of $PUSA_{100}$ and $PUSA_{100}$-PANI.PTSA.

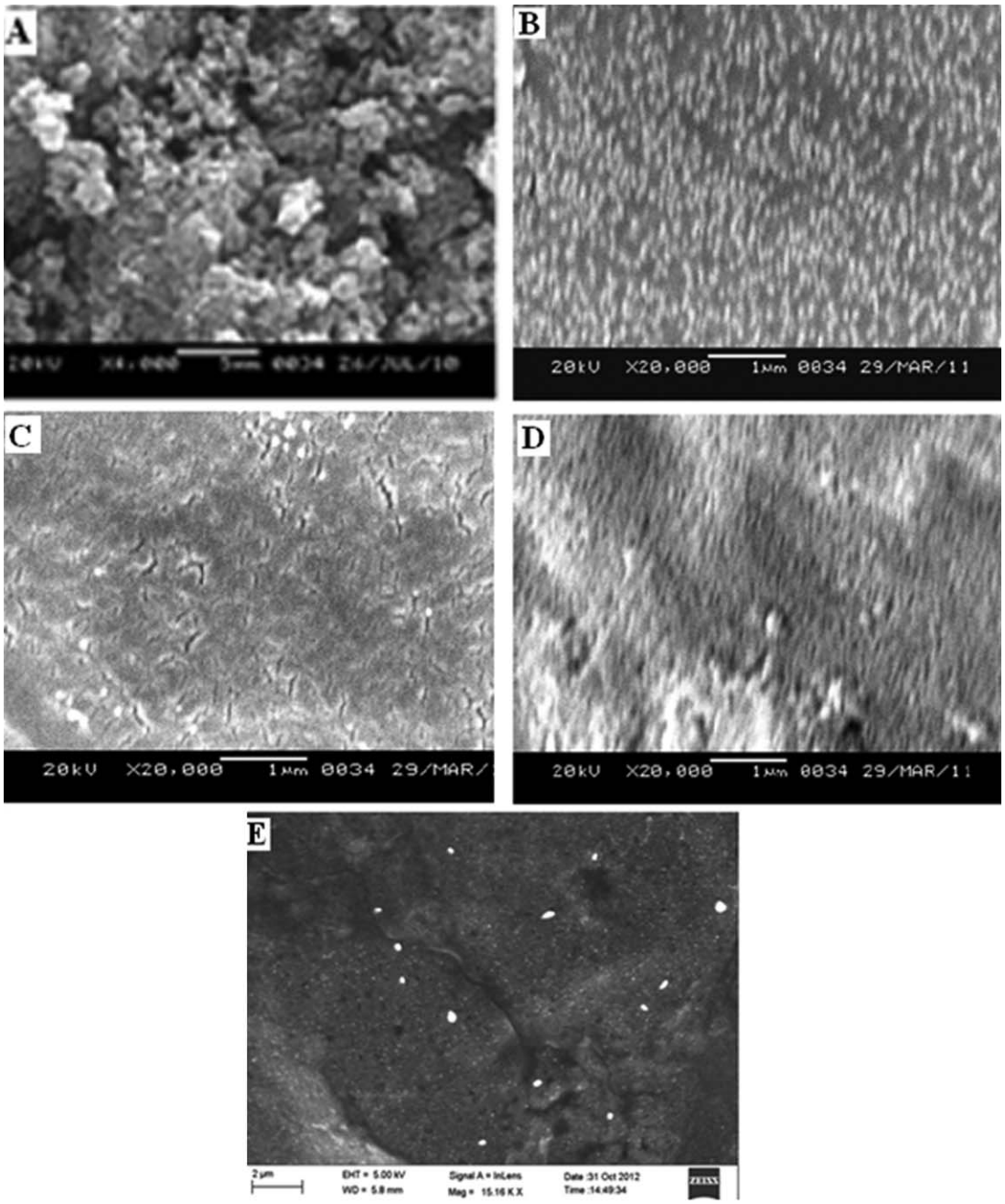

Figure 11. SEM images of (A) PANI.PTSA, (B) $PUSA_{100}$, (C) 1 wt % PANI.PTSA/$PUSA_{100}$ (D) 30 wt % PANI.PTSA/$PUSA_{100}$ composite and FESEM image of (E) 30 wt % PANI.PTSA/ $PUSA_{100}$ composite.

300–600°C (~50%) is due to a large scale thermal degradation of the PANI chains.[40–42] The terminal degradation temperature of PANI is 629°C with very little residue remaining under the experimental conditions.[43] The thermogram of PANI.PTSA/$PUSA_{100}$ is more similar to that of $PUSA_{100}$, but with an imprint of the PANI.PTSA thermogram. As the TGA-curves also serve a diagnostic purpose, the TGA-curves of the composite provides ample proof of formation of a new material different from the constituents. The thermogram of $PUSA_{100}$ and PANI.PTSA/$PUSA_{100}$ exhibit a very small initial weight loss (~4%) in the region of room temperature—270°C which may be attributed to the elimination of moisture. When 50% weight loss is selected as a point of comparison, the corresponding temperatures are found at 350°C, 370°C, and 325°C, respectively for PANI.PTSA, $PUSA_{100}$, and 30 wt % of PANI.PTSA/$PUSA_{100}$ composite. Further the TGA-traces reveals that loading of PANI changes the thermal behaviour of $PUSA_{100}$ and residual weight after major weight loss increased considerably.

Differential Scanning Calorimetry Studies

Figure 10 presents the low temperature DSC-traces of $PUSA_{100}$ and $PUSA_{100}$-PANI.PTSA composite. The glass transition

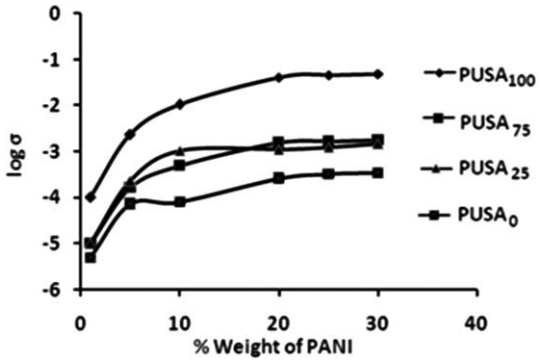

Figure 12. The room temperature electrical conductivity (σ) of PANI.PTSA/PUSA composites as a function of wt % of PANI.PTSA content.

temperature (T_g) of PUSA in the pristine form was observed at −34°C. The glass transition temperature shifts to −32°C in the composite. The marginal increase in the glass transition value of the PU-anionomer in the composite indicates little change in its flexibility in the composite.

Scanning Electron Microscopic Studies

The scanning electron microscopy and field emission SEM were used to investigate the effect of PANI.PTSA on the morphology of the PUSA composites. Figure 11 shows the SEM and FESEM images of PANI.PTSA and PANI.PTSA (1 and 30 wt %)/$PUSA_{100}$ composites. The SEM image of PANI.PTSA shows the presence of clusters of spherical particles. The two phase structure of PU ionomer $PUSA_{100}$ is visible in its SEM-image.[44] It is evident from the SEM-images that the presence of PANI.PTSA profoundly influences the morphology of the host PU anionomer. Even the presence of 1 wt % of PANI.PTSA makes perceptible change in the morphology of host $PUSA_{100}$. The dark region in the image is due to dispersed PANI.PTSA. The dark reasons are well connected with each other in the composites with 30 wt % of PANI.PTSA. This is more discernible in the FESEM image of the composite. This interconnectivity is the reason for the observed higher conductivity for the composite with 30 wt % of PANI.PTSA.

Electrical Conductivity

Figure 12 shows the room temperature electrical conductivity of PANI.PTSA/PUSA composites as a function of wt % of PANI.PTSA content, for three varieties of PUSA viz. $PUSA_{100}$, $PUSA_{75}$, and $PUSA_{25}$ along with the composite of PANI.PTSA/$PUSA_0$ for comparison. It is observed that the conductivity of the composites depends on two factors, the nature of the PU anionomer and the amount of PANI.PTSA in the composites. In three varieties of the composites, the conductivity increased with increasing PANI.PTSA content. It is however interesting to note that the % of ionic groups present in the PU anionomer has affected the conductivity. For the same PANI.PTSA content $PUSA_{100}$ composites having the highest percentage of ionic groups has the highest conductivity value. For 30 wt % of PANI.PTSA, the conductivity values are 4.921×10^{-2}, 1.762×10^{-3}, and 1.313×10^{-3} S cm^{-1} respectively for the composites of $PUSA_{100}$, $PUSA_{75}$ and $PUSA_{25}$ PU anionomers. So this could be safely stated that the anionic groups in the PU backbone interact with the positively charged PANI chains increasing the long range order in the arrangement of PANI chains and thereby facilitate the rise in the conductivity values. The conductivity of composites containing PU was always less than those containing PU anionomer, which further indicates the positive role played by the anionic groups on increase in conductivity values. For 30 wt % of PANI.PTSA, the conductivity value of PANI.PTSA/$PUSA_0$ was 3.422×10^{-4} S cm^{-1}. However, the highest conductivity (4.921×10^{-2} S cm^{-1}) for PANI.PTSA/$PUSA_{100}$ composite, which was observed for 30 wt % of PANI.PTSA, is much lower compared with PANI.PTSA (2.136×10^{-1} S cm^{-1}). The lower value of conductivity of composites compared to pristine PANI is due to the presence of an insulating matrix accounting for the reduction in the inter-chain hopping between PANI chains.[45] Vicentini and coworkers[25] reported the synthesis of a thermoplastic PU/PANI blend and observed a maximum electrical conductivity of 1.5×10^{-2} for 30 wt % PANI in the blend. Rodrigues and coworkers [46] reported blending of PU and PANI and observed a maximum conductivity 4×10^{-4} Scm^{-1} for the 30/70 PANI/PU ratios. The experimental data on the conductivity values could be fitted to the scaling law of percolation theory,[44,47] as described in equation $\sigma_f = c\ (f - f_p)^t$ where c is a constant, t is a critical exponent, σ_f the conductivity, f the fraction of conducting medium and f_p the fraction of percolation threshold, expressed in weight fraction. The plot of log σ versus log $(f - f_p)$ for the PANI.PTSA/$PUSA_{100}$ is shown in Figure 13. The percolation threshold and other parameters calculated through the plot of log σ verses log $(f - f_p)$ are shown in Table II. The values for the critical exponent were in the range of 2–4, which may be due to multiple percolation in conducting polymer composites as proposed by Levon and Margolina.[44] The f_p value is a reflection of compatibility between the conducting polymer and the

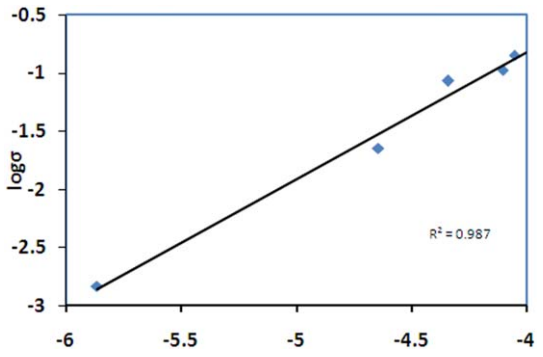

Figure 13. The plot of log σ versus log $(f - f_p)$ for the PANI.PTSA/$PUSA_{100}$. [Color figure can be viewed in the online issue, which is available at wileyonlinelibrary.com.]

Table II. Percolation Threshold Data for Composites of PUSA100, PUSA25, and PUSA0, Respectively

Ionomer	Percolation threshold (fp) (wt %)	Critical exponent	Correlation coefficient (*R*)
$PUSA_{100}$	1.5	1.9	0.984
$PUSA_{25}$	2	2	0.989
$PUSA_0$	2	2.278	0.993

matrix polymer. Vicentini et al.[25] reported that the low f_p value for PU–PANI–DBSA blend indicated a better compatibility due to the presence of carbonyl/amine group interactions. Our results indicated that the presence of anionic groups on the PUs enhances the compatibility further, resulting in the lowest f_p value for the $PUSA_{100}$–PANI composite.

CONCLUSION

The electrical conductivity of a blend or composite of conductive polymer and a non-conductive elastomeric polymer depends to a large extent on the nature of the matrix polymer and the compatibility between the two. Further simple solution mixing of the two polymer followed by casting are known to allow the formation of volume modified film composites with linear current–voltage characteristics.[48] We have successfully prepared films of PTSA-doped PANI and PUSAs. It was observed that the change of PU by PU anionomer resulted in an increase in conductivity by 10^2 fold, with concomitant lowering of percolation threshold. Further, it was observed that the conductivity of the films could be modulated by changing the % of ionic groups in the PU-anionomer. The TGA-analysis showed that the conductive films presented a thermal stability upto ~300°C. The DSC data revealed that the glass transition temperature of the PU-anionomer showed a little increase as a result of composite formation with PANI, indicating only minor change in the flexible nature of the matrix polymer. Overall we have demonstrated a simple method of preparation of conductive composite films of PTSA-doped PANI and PUSA having relatively good thermal stability.

REFERENCES

1. Gurunathan, K.; Amalnerkar, D. P.; Trivedi, D. *Mater. Lett.* **2003**, *57*, 642.
2. Janata, J.; Josowicz, M. *Nat. Mater.* **2003**, *2*, 19.
3. Skotheim, T. A.; Reynolds J. R. Ed. Handbook of Conducting Polymers, 3rd ed.; CRC Press: Boca Raton, Florida, **2007**.
4. Wang, Y.; Jing, X. *Polym. Adv. Tech.* **2005**, *16*, 344.
5. Dhawan, S. K.; Trivedi, D. C. *J. Appl. Polym. Sci.* **1995**, *58*, 815.
6. Wey, Y.; Focke, W. W.; Wnek, G. E. *J. Phys. Chem.* **1989**, *93*, 495.
7. Yue, J.; Epstein, A. J. *J. Am. Chem. Soc.* **1990**, *112*, 2800.
8. Shimizu, S.; Saitoh, T.; Uzawa, M.; Yuasa, M.; Yano, K.; Maruyama, T.; Watanabe, K. *Synth. Met.* **1997**, *85*, 1337.
9. Hwang, G. W.; Wu, K. Y.; Hua, M. Y.; Lee, H. T.; Chen, S. A. *Synth. Met.* **1998**, *92*, 39.
10. Bergeron, J. Y.; Chevalier, J. W.; Dao, L. H. *J. Chem. Soc., Chem. Commun.* **1990**, *2*, 180.
11. Chen, S. A.; Hwang, G. W. *J. Am. Chem. Soc.* **1995**, *117*, 10055.
12. Dearmitt, C.; Armes, S. P.; Winter, J.; Uribe, F. A.; Gottesfeld, S.; Mombourquette, C. A. *Polymer* **1993**, *34*,158.
13. Wang, P.; Tan, K. L.; Zhang, F.; Kang, E. T.; Neoh, K. G. *Chem. Mater.* **2001**, *13*, 581.
14. Chen, Y.; Kang, E. T.; Neoh, K. G.; Tan, K. L. *Polymer* **2000**, *41*, 3279.
15. Anand, J.; Palaniappan, S.; Sathyanarayana, D. N. *Prog. Polym. Sci.* **1998**, *23*, 993.
16. Pud, A.; Ogurtsov, N.; Korzhenko, A.; Shapoval, G. *Prog. Polym. Sci.* **2003**, *28*, 1701.
17. Petrovic, Z. S.; Ferguson, J. *Prog. Polym. Sci.* **1991**, *16*, 695.
18. Malmonge, J. A.; Campoli, C. S.; Malmonge, L. F.; Kanda, D. H. F.; Mattoso, L. H. C.; Chierice, G. O. *Synth. Met.* **2001**, *119*, 87.
19. Aboutanos, V.; Kane-Maguire, L. A. P.; Wallace, G. G. *Synth. Met.* **2000**, *114*, 313.
20. Rodrigues, P. C.; Akcelrud, L. *Polymer* **2003**, *44*, 6891.
21. Rodrigues, P. C.; Lisboa-Filho, P. N.; Mangrich, A. S.; Akcelrud, L. *Polymer* **2005**, *46*, 2285.
22. Abbati, G.; Carone, E.; D'llario, L.; Martinelli, A. *J. Appl. Polym. Sci.* **2003**, *89*, 2516.
23. Kwon, J. Y.; Kim, E. Y.; Kim, H. D. *Macromol. Res.* **2004**, *12*, 303.
24. Sapurina, I.; Stejskal, J.; Sprkova, M.; Kotek, J.; Prokes, J. *Synth. Met.* **2005**, *15*, 93.
25. Vicentini, D. S.; Barra, G. M. O.; Bertolino, J. R.; Pires, A. T. N. *Eur. Polym. J.* **2007**, *43*, 4565.
26. Chien-Yu, L.; Chiu, W. Y.; Don, T. M. *J. Polym. Sci. A Polym. Chem.* **2007**, *45*, 3902.
27. Chiou, W. C.; Yang, D. Y.; Han, J. L.; Lee, S. N. *J. Polym. Int.* **2006**, *55*, 1222.
28. Chiou, W. C.; Han, J. L.; Lee, S. N. *Polym. Eng. Sci.* **2008**, *48*, 345.
29. Gurunathan, T.; Rao, C. R. K.; Narayan, R.; Raju, K. V. S. N. *J. Mater. Sci.* **2013**, *48*, 67.
30. Chui, T. Y. T.; Lam, P. K. H.; George, M. H.; Barrie, J. A. *Polym. Commun.* **1988**, *29*, 317.
31. Lam, P. K. H.; George, M. H.; Barrie, J. A. *Polymer* **1989**, *30*, 2320.
32. Ramesh, S.; Ganga, R. *Polymer* **1994**, *35*, 3107.
33. Kakati, D. K.; George, M. H. *Polymer* **1994**, *53*, 398.
34. Cao, Y.; Smith, P.; Heeger, A. *Synth. Met.* **1992**, *48*, 91.
35. Armarego, W. L. F.; Chai, C. L. L. Purification of Laboratory Chemicals, 6th ed.; Butterworth–Heinemann: Jordan Hill, Oxford, UK, **2008**.
36. Hrehorova, E.; Bliznyuk, V. N.; Pud, A. A.; Shevchenko, V. V.; Fatyeyeva, K. Y. *Polymer* **2007**, *48*, 4429.
37. Goncalves, D.; Waddon, A.; Karasz, F. E.; Akcelrud, L. *Synth. Met.* **1995**, *74*, 197.
38. Tang, J.; Jing, X.; Wang, B.; Wang, F. *Synth. Met.* **1988**, *24*, 231.
39. Lesueur, D.; Colin, X.; Camino, G.; Alberola, N. D. *Polym. Bull.* **1997**, *39*, 755.
40. Xuan, S. H.; Wang, Y. X. J.; Leung, K. C. F.; Shu, K. *J. Phys. Chem. C* **2008**, *112*, 18804.
41. Feng, X.; Mao, C.; Yang, G.; Hou, W.; Zhu, J. *Langmuir* **2006**, *22*, 4384.
42. Trchová, M.; Konyushenko, E. N.; Stejskal, J.; Kovárová, J.; Ciric-Marjanovic, G. *Polym. Degrad. Stab.* **2009**, *94*, 929.

43. Gu, H.; Huang, Y.; Zhang, X.; Wang, Q.; Zhu, J.; Shao, L.; Haldolaarachchige, N.; Young, D. P.; Wei, S.; Guo, Z. *Polymer* **2012**, *53*, 801.
44. Levon, K.; Margolina, A. *Macromolecules* **1993**, *26*, 4061.
45. Dutta, P.; Dey, S. K. *Synth. Met.* **2003**, *139*, 201.
46. Rodrigues, P. C.; Souza, G. P.; da Motta, J. D.; Akcelrud, L. *Polymer* **2002**, *43*, 5493.
47. Stauffer, D.; Aharony, A. Introduction to Percolation Theory, 2nd ed. Taylor and Francis: London, **2010**.
48. Hrehorova, E.; Bliznyuk, V. N.; Pud, A. A.; Shevchenko,V. V.; Fatyeyeva, K. Y. *Polymer* **2007**, *48*, 4429.